Project Report
ATC-223

Obtaining Low Sidelobes Using Non-Linear FM Pulse Compression

M. Labitt

4 November 1994

Lincoln Laboratory
MASSACHUSETTS INSTITUTE OF TECHNOLOGY
LEXINGTON, MASSACHUSETTS

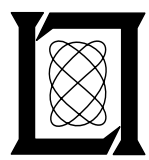

Prepared for the Federal Aviation Administration,
Washington, D.C. 20591

TECHNICAL REPORT STANDARD TITLE PAGE

1. Report No.	2. Government Accession No.	3. Recipient's Catalog No.
ATC-223		

4. Title and Subtitle	5. Report Date
Obtaining Low Sidelobes Using Non-Linear FM Pulse Compression	4 November 1994
	6. Performing Organization Code
7. Author(s)	8. Performing Organization Report No.
Melvin Labitt	ATC-223
9. Performing Organization Name and Address	10. Work Unit No. (TRAIS)
Lincoln Laboratory, MIT P.O. Box 73 Lexington, MA 02173-9108	11. Contract or Grant No. DTFA01-93-Z-02012
12. Sponsoring Agency Name and Address	13. Type of Report and Period Covered
Department of Transportation Federal Aviation Administration Systems Research and Development Service Washington, DC 20591	Project Report
	14. Sponsoring Agency Code

15. Supplementary Notes

This report is based on studies performed at Lincoln Laboratory, a center for research operated by Massachusetts Institute of Technology. The work was sponsored by the Air Force under Contract F19628-95-C-0002.

16. Abstract

Airport Surveillance Radar (ASR) manufacturers are proposing the use of non-linear FM pulse compression in their all solid state radars. However there is concern that the use of pulse compression will limit the radar's performance. High range sidelobes can cause poor performance in both target and weather detection.

The theory of non-linear FM pulse compression is derived along with a method of minimizing the sidelobes using a minimum mean square error (MMSE) technique. The results of a computer program using the MMSE technique show that very low sidelobe levels of more than 100 dB down may be achieved. These very low sidelobes are affected by filter misalignment, target Doppler, and by transmitter phase errors or stability. Curves are presented demonstrating these effects. We also show how filter misalignment can be corrected by receiver filtering. The methods presented here are general enough to be used to assess the performance of proposed non-linear FM waveform radars.

17. Key Words		18. Distribution Statement
pulse compression non-linear FM	ASR low sidelobes	This document is available to the public through the National Technical Information Service, Springfield, VA 22161.

19. Security Classif. (of this report)	20. Security Classif. (of this page)	21. No. of Pages	22. Price
Unclassified	Unclassified	33	

FORM DOT F 1700.7 (8-72) Reproduction of completed page authorized

ABSTRACT

Airport Surveillance Radar (ASR) manufacturers are proposing the use of non-linear FM pulse compression in their all solid state radars. However there is concern that the use of pulse compression will limit the radar's performance. High range sidelobes can cause poor performance in both target and weather detection.

The theory of nonlinear FM pulse compression is derived along with a method of minimizing the sidelobes using a minimum mean square error (MMSE) technique. The results of a computer program using the MMSE technique show that very low sidelobe levels of more than 100 dB down may be achieved. These very low sidelobes are affected by filter misalignment, target Doppler, and by transmitter phase errors or stability. Curves are presented demonstrating these effects. We also show how filter misalignment can be corrected by receiver filtering. The methods presented here are general enough to be used to assess the performance of proposed non-linear FM waveform radars.

TABLE OF CONTENTS

LIST OF ILLUSTRATIONS

LIST OF TABLES

1. Introduction

Many Airport Surveillance Radar (ASR) manufacturers are proposing the use of pulse compression in their all solid state candidate radars as a means to improve reliability. However there is concern about how well these systems will compare with conventional uncompressed radars. Specifically, compressed waveforms have time sidelobe levels that vary with the matched filter design, the target Doppler velocity, and other parameters. These varying sidelobe levels must be characterized and understood for a proper assessment of the target and weather detection capability of a proposed radar design.

The theory of nonlinear frequency modulation of pulse compression is derived and the results of numerical calculations are presented here. Achievable time sidelobe levels, Doppler effects, filter misalignment, phase errors, and mismatch losses will be calculated and/or discussed.

2. Transmitted Waveform

2.1 Principle of Stationary Phase

We will show here how an almost ideal transmitted waveform is derived from an arbitrary spectrum. This is useful because the compressed pulse shape is the autocorrelation function of the transmitted waveform which in turn is the Fourier transform of the spectrum. This method is due to Fowle[1].

The complex transmitted waveform $u(t)$ is related to its complex spectrum $U(f)$ by the Fourier transform

$$u(t) = \int_{-\infty}^{\infty} U(f)e^{-i2\pi ft}df = \int_{-\infty}^{\infty} U_m(f)e^{\theta(f)}e^{-i2\pi ft}df \tag{1}$$

where $U_m(f)$ and $\theta(f)$ are the magnitude and phase of the spectrum.

$$u(t) = \int_{-\infty}^{\infty} U_m(f)e^{i[\theta(f)-2\pi ft]}df \tag{2}$$

The principle of stationary phase states that when

$$\frac{d}{df}[\theta(f) - 2\pi ft] = 0 \tag{3}$$

the largest contribution to the integral (1) occurs in this region. Thus

$$\theta'(f) - 2\pi t = 0 \tag{4}$$

Let us expand $[\theta(f) - 2\pi ft]$ using the first three terms of a Taylor series around f_k:

$$\theta(f) - 2\pi ft = (\theta(f_k) - 2\pi f_k t) + [\theta'(f_k) - 2\pi t)](f - f_k) + \frac{\theta''}{2}(f - f_k)^2 \tag{5}$$

The second term is zero thus Eq(2) becomes

$$u(t) = \int_{f_k-\delta}^{f_k+\delta} U_m(f_k)e^{i[\theta(f_k)-2\pi f_k t+\frac{\theta''(f_k)}{2}(f-f_k)^2]}df. \tag{6}$$

Moving the constant factors outside of the integral we find

$$u(t) = e^{i[\theta(f_k)-2\pi f_k t]} U_m(f_k) \int_{f_k-\delta}^{f_k+\delta} e^{i[\frac{\theta''(f_k)}{2}(f-f_k)^2]} df. \tag{7}$$

To evaluate the integral we make the following substitutions

$$\mu = f - f_k \tag{8}$$

and

$$\frac{\theta''}{2}\mu^2 = \frac{\pi y^2}{2}. \tag{9}$$

Thus Eq(7) becomes

$$u(t) = U_m(f_k) e^{[\theta(f_k)-2\pi f_k t]} \sqrt{\frac{\pi}{\theta''(f_k)}} \int_{-\sqrt{\frac{\theta''(f_k)}{\pi}}\delta}^{\sqrt{\frac{\theta''(f_k)}{\pi}}\delta} e^{i[\frac{\pi y^2}{2}]} dy \tag{10}$$

If we take the magnitude and let $\delta \rightarrow \infty$ we find

$$u_m(t) = U_m(f_k) \frac{\sqrt{\pi}}{\sqrt{\theta''(f_k)}} \left| \int_{-\infty}^{\infty} e^{i\frac{\pi y^2}{2}} dy \right| \tag{11}$$

Separating into real and imaginary parts, we have

$$u_m(t) = U_m(f_k) \frac{\sqrt{\pi}}{\sqrt{\theta''(f_k)}} \left| \int_{-\infty}^{\infty} \cos(\frac{\pi y^2}{2}) dy + i \int_{-\infty}^{\infty} \sin(\frac{\pi y^2}{2}) dy \right|. \tag{12}$$

The integrals are the cosine and sine Fresnel integrals and each are equal to one. Taking the square and dropping the subscript k we have

$$u_m^2 = U_m^2(f) \frac{2\pi}{\theta''(f)} \tag{13}$$

If we differentiate Eq(4) with respect to f we find

$$\theta''(f) = 2\pi \frac{dt}{df} \tag{14}$$

Substituting into Eq(13) we finally obtain

$$u_m^2(t)dt = U_m^2(f)df. \tag{15}$$

If we integrate Eq(15) from $-\infty$ to $+\infty$ we will have Parseval's law. We will instead form the general integral

$$\int_{-t}^{t} u_m^2(\eta)d\eta = \int_{-f}^{f} U_m^2(\xi)d\xi \tag{16}$$

from which we can obtain $f(t)$.

2.2 Transmitter Waveform Generation

Note that in Eq(16) we are dealing with a transmitted pulse power $u_m^2(t)$ and a spectral power $U_m^2(f)$. In order to have good efficiency in a solid state transmitter, a constant power (square pulse) should be used.

$$u_m^2(\eta) = \frac{1}{T} \qquad \left[-\frac{T}{2} \leq \eta \leq \frac{T}{2}\right] \tag{17}$$

$U_m^2(\xi)$ is chosen to have finite bandwidth and to taper to zero on each side. These types of functions are well known in antenna theory.

An evaluation of $f(t)$ when $U_m^2(\xi) = \cos^2(\frac{\pi\xi}{2B})$ and $u_m^2(\eta) = \frac{1}{T}$ is now shown. Using normalized functions in Eq(16), we have

$$\frac{1}{T}\int_{-t}^{t} d\eta = \frac{2}{B}\int_{-f}^{f} \cos^2(\pi\frac{\xi}{B})d\xi \tag{18}$$

or

$$t = T\left(\frac{\sin\left(\frac{2\pi f}{B}\right)}{2\pi} + \frac{f}{B}\right) \qquad \left[-\frac{B}{2} \leq f \leq \frac{B}{2}\right] \tag{19}$$

We now have the inverse function $t(f)$ and will employ numerical methods to obtain $f(t)$ from which we generate the phase function

$$\phi(t) = 2\pi \int_0^t f(\eta) d\eta, \tag{20}$$

and the transmitted waveform will be

$$u(t) = \frac{1}{\sqrt{T}} e^{i\phi(t)} \qquad \left[-\frac{T}{2} \leq t \leq \frac{T}{2}\right]. \tag{21}$$

Since we will be using digital processing, time will be quantized, $t = n\Delta T$, and the unnormalized transmitter waveform will be approximated by the sequences

$$b_n = e^{i\phi(n\Delta T)} \qquad n = 0, 1, 2 \ldots M-1 \tag{22}$$

$$b_n = 0 \qquad n \neq 0, 1, 2 \ldots M-1 \tag{23}$$

where n is an integer and ΔT is transmitter interpulse spacing.

The $\cos^2(\frac{\pi f}{2B})$ spectrum was chosen for the following reasons: (1) The bandwidth is finite; (2) The time sidelobes will be small so that additional processing will be a small correction approaching a low loss matched filter; (3) The Fourier transform is well known from antenna theory. The conjugate of b_n would be the obvious filter waveform to process b_n. The output of the filter would be the convolution

$$a(n) = b^* \otimes b(n)$$

where $\otimes$ is the convolution symbol. Thus we have

$$a(n) = \sum_{s=0}^{N-1} b_n^* b(s-n) \qquad n = 0, 1 \ldots 2N-2. \tag{24}$$

$a(n)$ is plotted in Figure (1) when $N = 2000$. It looks similar to a cosine weighted antenna pattern.

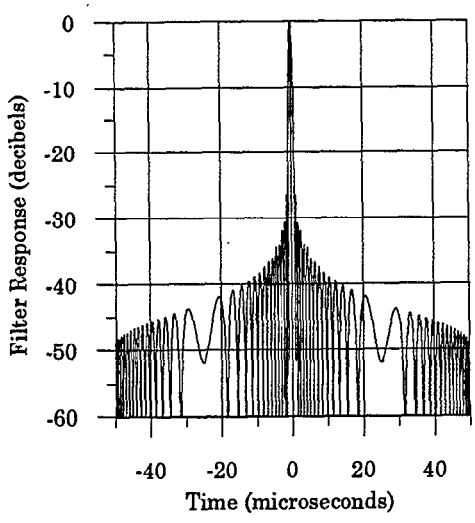

Figure 1. Time sidelobes for a matched filter derived from a cosine squared spectrum.

3. Mean Square Error Reduction of Sidelobes

Consider the possibility of reducing the time sidelobes obtained in Figure (1) by modifying the receiver filter which is now the conjugate of $b(n)$. The modification will be small because $f(t)$ already produces low sidelobes. Thus the resultant filter will be nearly matched and have low losses.

A minimum mean square error filter also known as a Weiner shaping filter[2] to reduce the sidelobes will be described here. Assume that the filter[1] $f(n)$ has M points. Then the filter output is the convolution

$$c(n) = b(n) \otimes f(n)$$

$$c(n) = \sum_{s=0}^{M-1} f(s)b((n-s) \qquad [n = 0,1,2 \ldots M+N-2] \tag{25}$$

Let $d(n)$ represent the ideal or wanted filter response. Since the main lobe of an antenna pattern can be approximated by a Gaussian curve, we will use

$$d(n) = e^{-k(n-\frac{M+N-2}{2})^2} \qquad [n = 0,1 \ldots M+N-2] \tag{26}$$

It is convenient to express k in terms of the pulse width τ. It can easily be shown that $k = \left(\frac{\Delta T}{\tau}\right)^2 \ln 4$ at the 3 dB pulse width of (26). τ is the desired pulse length. The error energy I is given by

$$I = \sum_{n=0}^{M+N-2} |e(n)|^2 = \sum_{n=0}^{M+N-2} |d(n) - c(n)|^2 \tag{27}$$

$$I = \sum_{n=0}^{M+N-2} \left| d(n) - \sum_{s=0}^{M-1} f(s)b(n-s) \right|^2 \tag{28}$$

Expanding we have

$$I = \sum_{n=0}^{M+N-2} \left(d(n) - \sum_{s=0}^{M-1} f(s)b(n-s) \right) \left(d^*(n) - \sum_{k=0}^{M-1} f^*(k)b^*(n-k) \right) \tag{29}$$

---

[1]Note that $f(t)$ is a frequency function while $f(n)$ is a filter coefficient.

where * is the complex conjugate. Taking the partial derivative with respect to $f^*(k)$ and setting it equal to 0 we have

$$\frac{\partial I}{\partial f^*(k)} = \sum_{n=0}^{M+N-2} \left(d(n) - \sum_{s=0}^{M-1} f(s) b(n-s) \right) (-b^*(n-k)) = 0 \tag{30}$$

where

$$k = 0, 1, 2 \ldots M-1.$$

Rearranging we find

$$\sum_{n=0}^{M+N-2} d(n) b^*(n-k) = \sum_{n=0}^{M+N-2} \sum_{s=0}^{M-1} f(s) b(n-s) b^*(n-k).$$

Summing the right side over n first, we have

$$\sum_{n=0}^{M+N-2} d(n) b^*(n-k) = \sum_{s=0}^{M-1} f(s) \sum_{n=0}^{M+N-2} b(n-s) b^*(n-k), \tag{31}$$

again remembering that we have M simultaneous equations when we range k.

$$k = 0, 1, 2 \ldots M-1.$$

To simplify things we let

$$g(k) = \sum_{n=0}^{M+N-2} d(n) b^*(n-k) \tag{32}$$

and

$$r(k-s) = \sum_{n=0}^{M+N-2} b(n-s) b^*(n-k). \tag{33}$$

Substituting (32) and (33) into (31) we obtain

$$g(k) = \sum_{s=0}^{M-1} f(s) r(k-s). \tag{34}$$

$$[k = 0, 1, 2 \ldots M-1]$$

We can visualize (34) by using matrix notation

$$\begin{bmatrix} r(0) & r^*(1) & r^*(2) & \cdots & r^*(M-1) \\ r(1) & r(0) & r^*(1) & \cdots & r^*(M-2) \\ r(2) & r(1) & r(0) & \cdots & r^*(M-3) \\ \vdots & \vdots & \vdots & \ddots & \vdots \\ r(M-1) & r(M-2) & r(M-3) & \cdots & r(0) \end{bmatrix} \begin{bmatrix} f(0) \\ f(1) \\ f(2) \\ \vdots \\ f(M-1) \end{bmatrix} = \begin{bmatrix} g(0) \\ g(1) \\ g(2) \\ \vdots \\ g(M-1) \end{bmatrix} \tag{35}$$

or symbolically

$$\boldsymbol{R}\boldsymbol{f} = \boldsymbol{g}. \tag{36}$$

We could solve for the filter coefficients using

$$\boldsymbol{f} = \boldsymbol{R}^{-1}\boldsymbol{g} \tag{37}$$

where $\boldsymbol{R}^{-1}$ is the inverse of $\boldsymbol{R}$. However it is not necessary to invert $\boldsymbol{R}$. Because $\boldsymbol{R}$ is Toeplitz, that is, all the diagonal elements are equal, special algorithms[3] are available that will significantly reduce the computer time needed to solve (34).

Once we find the filter values $f(n)$ we can test our results using (25) to obtain the time sidelobe response to a point target.

4. Results

The examples chosen here are meant to be applicable to an Airport Surveillance Radar(ASR). The transmitter is solid state, and to be efficient, is only phase modulated as in (22). The first case shown has 201 points in the transmitted waveform which are spaced .25 μseconds apart. The receiver filter will also have 201 points spaced .25 μseconds apart. The radar parameters are listed in Table 1. The results using the minimum mean square error (MMSE) technique is shown in Figure 2. The sidelobes are not much better than what was obtained without using MMSE. Compare with Figure 1. Apparently there are not enough degrees of freedom to allow the proper reduction of sidelobes.

TABLE 1

Radar Parameters.

Compressed pulse width	1 μsec
Transmitted pulse length	50 μsec
Transmitted amplitude modulation	none
Transmitted waveform	Eq (22)
Total bandwidth B	1.6 MHz
Number of transmitted samples N	201
Transmitter sampling period	.25 μsec
Number of filter points M	201

4.1 MMSE Solution when M $\gg$ N, Filter Misalignment

The filter length M is now increased to provide more degrees of freedom. A Minimum Mean Square Error solution where $M = 1401$ and $N = 201$ is shown in Figure 3. It appears that we have achieved very low sidelobes, more than 103 dB. In the region ± 50 μsec we have better than 175 dB. Compare with Figure 2. However there is a problem. What one sees in Figure 3 is the result of sliding the filter (or the target) one point (ΔT) at a time. The points in this example are .25 μsecs apart. A real radar target moves continuously and in general will generate a return that will arrive in between these selected points. Figure 4 shows what happens when intermediate points

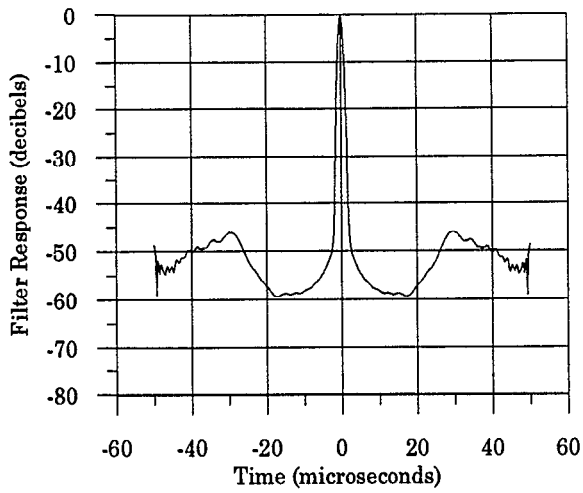

Figure 2. Time sidelobes minimum mean square error filter. Case where the receiver filter length equals transmitted sequence length. $M = N$.

are used.[2] The blackened areas are oscillations. If one traces out the minimum of these oscillations one obtains Figure 3. The oscillations can be seen in detail by expanding the graph as in Figure 5. The worst case occurs when the filter points lie somewhere between the transmitter $b(n)$ points.

4.2 Receiver Narrow Banding.

A problem occurs when calculating the interpolated points. Assume there are N points in the transmitted sequence. The interpolated sequence can only contain $N-1$ points because the $b(n)$ function is undefined outside the region $n = 0, 1 \ldots N-1$. Thus we have lost one of the points whenever we attempt to do the interpolation calculation. This accounts for the poor sidelobe performance of Figure 4. In the real world, the receiver has a finite band-width which will lengthen the sequence and can provide energy for the missing point. The solution is to narrow band the receiver by running the signal through a simple digital smoothing filter. This will ensure that when sampling is performed in the space lying between the original set of points the signal will not change

[2]The calculation is performed by generating a transmitter waveform having J intermediate points. Figure 4 is the result of convolving $f(n)$ with $b_j(n)$ where the subscript j represents the offset of the interpolated points, $n = 0, 1 \ldots N-1$, and $j = 0, 1 \ldots J$. J is a small number such as 1,2 or 4.

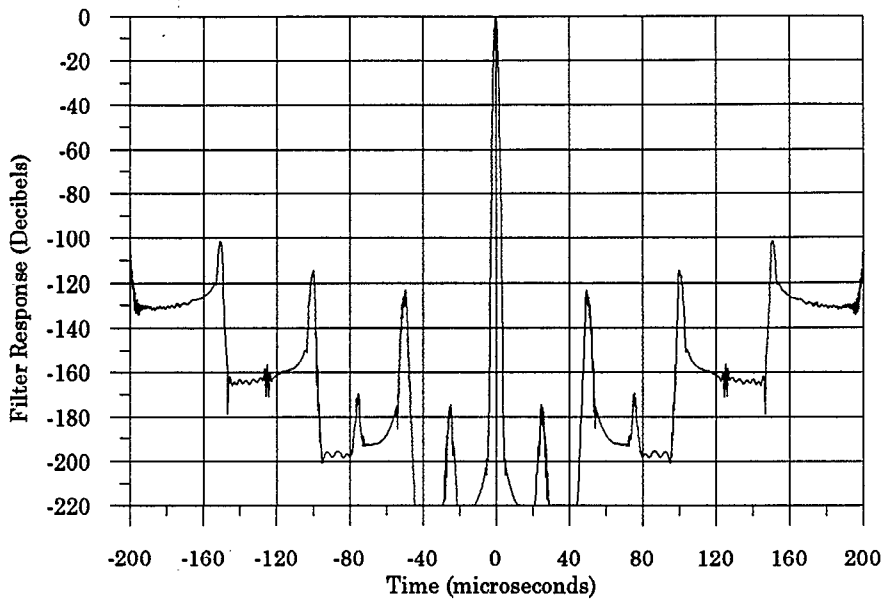

Figure 3. Time sidelobes minimum mean square error filter. Case where filter length is much larger than the transmitted sequence. $M = 1401$. $N = 201$.

very much. First let us start with a fine structured sequence that has p times as many points to more accurately represent the transmitted waveform than (22),

$$b_f(r) = e^{i\phi(\frac{r\Delta T}{p})}, \tag{38}$$

where

$$r = 0, 1, \cdots, pN-1,$$

and where p is an integer usually having a value of 2, 4, or 8. b_f is first convolved with a weighting filter $a(s)$ to slow the rise and fall times and then decimated to produce

$$b'(n) = \sum_{s=0}^{S-1} a(s) b_f(pn - s). \tag{39}$$

$$n = 0, 1, \cdots, S+N-1$$

The smoothing weights are the binomial coefficients

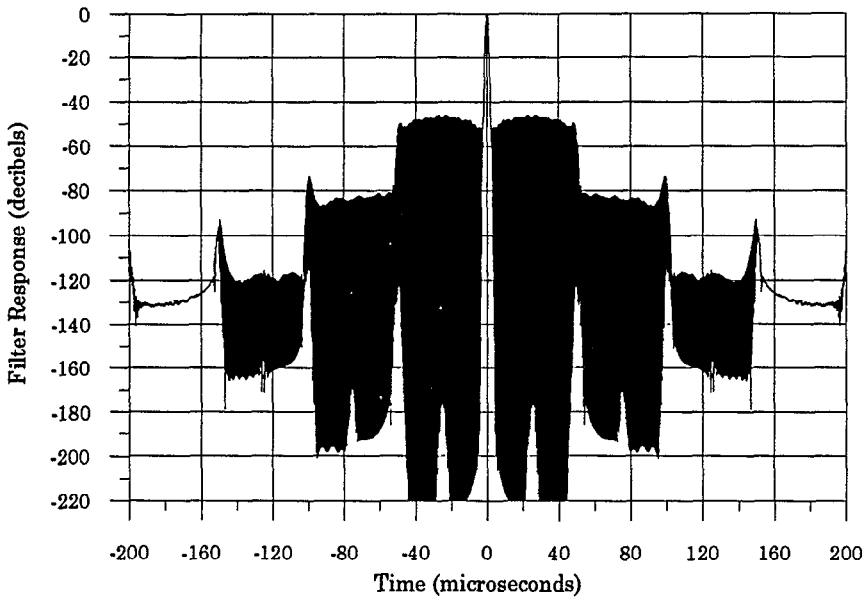

Figure 4. Time sidelobes minimum mean square error filter. Intermediate points calculation. The blackened areas are fine structured oscillations. The bottom edge of the blackened areas correspond to the curve in Figure 3. $M = 1401$. $N = 201$.

$$a(s) = \frac{S!}{(S-s)!s!}. \tag{40}$$

A plot of the amplitude of $b'(n)$ is shown in Figure 6. The MMSE filter is calculated from b'. The transmitted waveform is still the same as before. It has a constant amplitude with an abrupt turn on and turn off. The smoothing filter will slow down the rise and fall time of the signal when it enters the receiver. Unfortunately the smoothing process mismatches the receiver and causes a loss in sensitivity. Thus it becomes a trade-off between low side lobes and sensitivity. A smoothed waveform should be less affected from misalignment.

Figure 7 shows the effect of smoothing using a $S = 33$ point binomial weighting. The time sidelobes are now at -110 dB peak.

4.3 Filter Mismatch Loss

When the receiver filter is not optimumly matched to the transmitter waveform a loss occurs. The main lobe of the of filter output time series is generally not as large as when the filter is

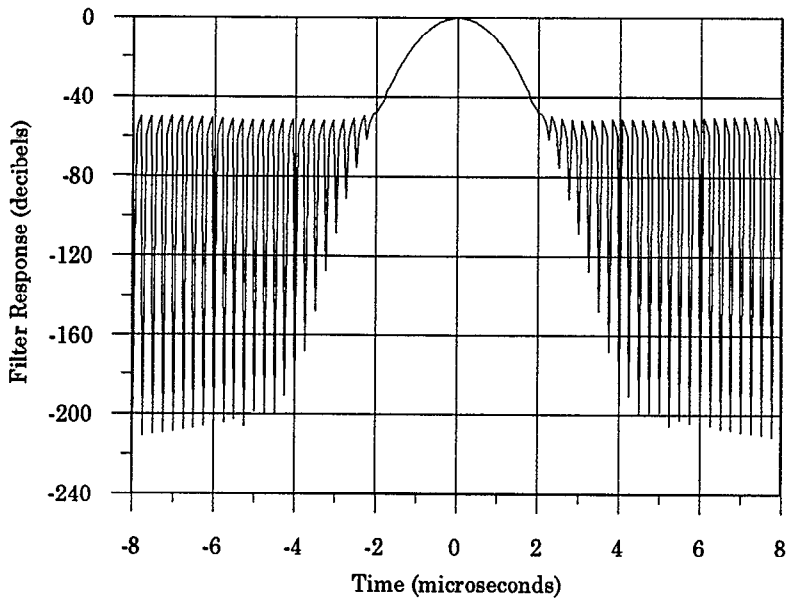

Figure 5. Expansion around the main lobe of Figure 4. Oscillation details are seen. Intermediate points calculation. $M = 1401$. $N = 201$.

matched. Consider the nonmatched case where the vector $\boldsymbol{w}^*$ is the filter operating upon a signal vector $\boldsymbol{s}$,

$$c = \sum_j w_j^* s_j = \boldsymbol{w}^* \boldsymbol{s}. \tag{41}$$

Schwartz's inequality states that

$$|\boldsymbol{w}^* \boldsymbol{s}|^2 \leq \boldsymbol{w}^* \boldsymbol{w} \cdot \boldsymbol{s}^* \boldsymbol{s}. \tag{42}$$

The equality occurs when $\boldsymbol{s} = \boldsymbol{w}$ and represents the matched filter case. Thus the function

$$r = \frac{|\boldsymbol{w}^* \boldsymbol{s}|^2}{\boldsymbol{w}^* \boldsymbol{w} \cdot \boldsymbol{s}^* \boldsymbol{s}} \leq 1 \tag{43}$$

is the mismatch of the filter and the mismatch loss L in dB is

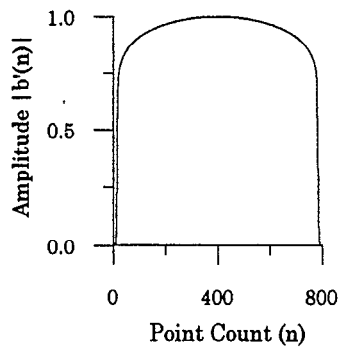

Figure 6. Amplitude $|b'(n)|$ of the received transmitter pulse. The rounded shoulders are from the narrow banding of the fast changing ends of the chirp pulse by the receiver.

$$L = -20\log_{10}\frac{|\boldsymbol{w}^*\boldsymbol{s}|^2}{\boldsymbol{w}^*\boldsymbol{w}\cdot\boldsymbol{s}^*\boldsymbol{s}}. \tag{44}$$

Figure 8 shows how the loss in detectability varies with the target Doppler velocity.

4.4 Doppler Sidelobe Deterioration

Non-linear FM time sidelobes will increase with increasing Doppler velocity of the target signal. A linear phase shift across the received signal was added to the computer program to simulate moving targets . This was implemented by the following replacement

$$b_f(n)e^{i2n\pi f_d\Delta T} \rightarrow b_f(n) \tag{45}$$

where n is the sequencing index and f_d is the Doppler frequency. Figure 9 shows how the time side lobes vary with target velocity. The maximum and integrated side lobe levels as a function of Doppler velocity are plotted. The integrated side lobe level is defined as the total power in the side lobes. These curves contain multiple points. The linearity of the curves is not understood. One would expect the curves to eventually level off at both high and low Doppler velocities. At low velocities the sidelobes will asymptotically level out to the zero Doppler case, while at high velocities the sidelobes will be energy limited and will level out somewhere below the main lobe level.

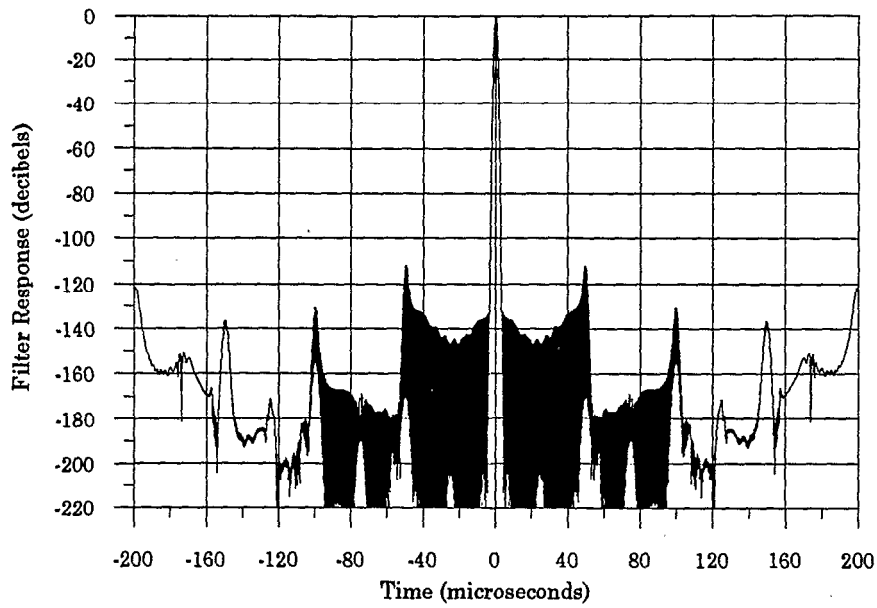

Figure 7. Low sidelobes obtained using 33 point binomial weighted smoothing. Intermediate points calculation. $M = 1401$. $N = 201$.

4.5 Phase Error Sidelobe Deterioration

Figure 10 similarly shows what happens when a random phase error in the transmitter waveform is introduced. Uncorrelated Gaussian phase noise is added point by point to the transmitted waveform. Also shown is the equivalent transmitter stability. The transmitter stability is related to phase noise in the following manner. Let the transmitter normalized output be represented by $1 + i\theta$ where θ is a Gaussian variate. The stability is defined as the AC power or variance divided by the total power. The total power is unity. The stability Γ in dB is

$$\Gamma = 10 \log_{10} \left[\frac{\mathrm{var}(1 + i\theta)}{1} \right]. \tag{46}$$

The variance is defined as the expected value of the square of the variate minus its mean.

$$\mathrm{var}(1 + i\theta) = \mathrm{E}\{(1 + i\theta - 1)^2\} = \mathrm{E}\{\theta^2\} \tag{47}$$

We therefore obtain the simple result

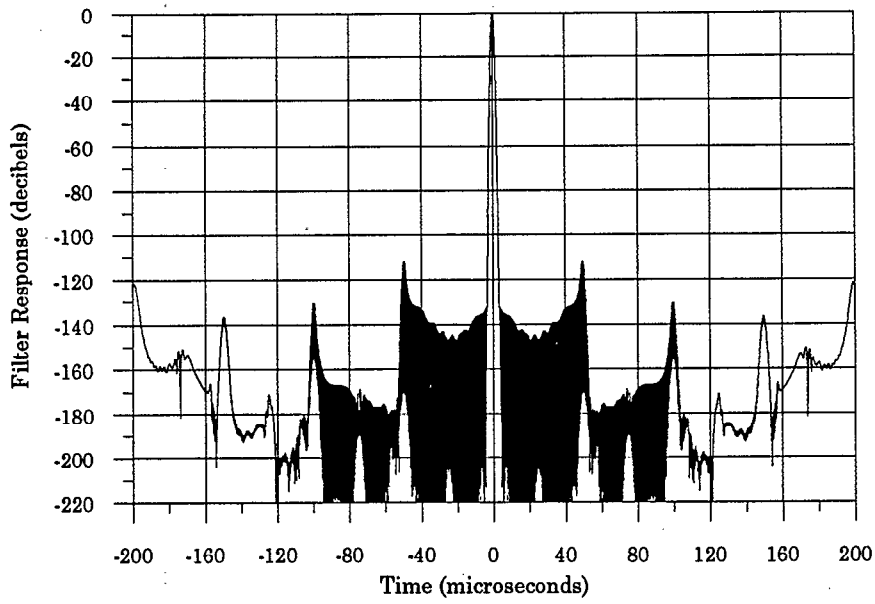

Figure 7. Low sidelobes obtained using 33 point binomial weighted smoothing. Intermediate points calculation. $M = 1401$. $N = 201$.

4.5 Phase Error Sidelobe Deterioration

Figure 10 similarly shows what happens when a random phase error in the transmitter waveform is introduced. Uncorrelated Gaussian phase noise is added point by point to the transmitted waveform. Also shown is the equivalent transmitter stability. The transmitter stability is related to phase noise in the following manner. Let the transmitter normalized output be represented by $1 + i\theta$ where θ is a Gaussian variate. The stability is defined as the AC power or variance divided by the total power. The total power is unity. The stability Γ in dB is

$$\Gamma = 10 \log_{10} \left[\frac{\mathrm{var}(1 + i\theta)}{1} \right]. \tag{46}$$

The variance is defined as the expected value of the square of the variate minus its mean.

$$\mathrm{var}(1 + i\theta) = \mathrm{E}\{(1 + i\theta - 1)^2\} = \mathrm{E}\{\theta^2\} \tag{47}$$

We therefore obtain the simple result

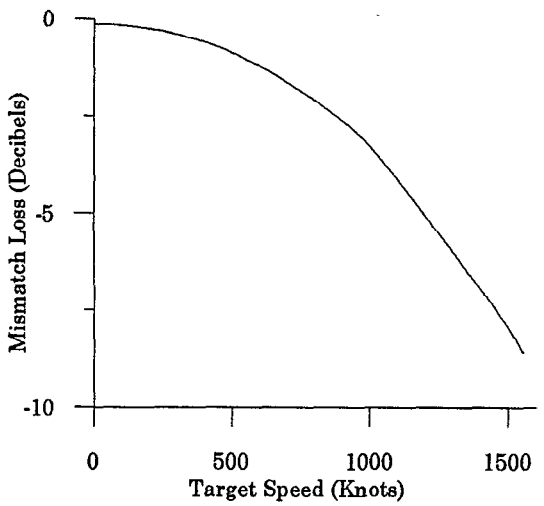

Figure 8. Mismatch loss L as a function of target velocity. 33 point binomial weighted smoothing. Intermediate points calculation. $M = 1401$. $N = 201$.

$$\Gamma = 20 \log_{10} \left(\frac{\pi}{180} \cdot \theta_{rms} \right) \tag{48}$$

where

$$\theta_{rms} = \frac{180}{\pi} \sqrt{\mathrm{E}\{\theta^2\}}$$

is the rms phase noise in degrees. Again we have a linear plot over this limited region. One would expect, as in the Doppler case, that leveling out will occur for similar reasons.

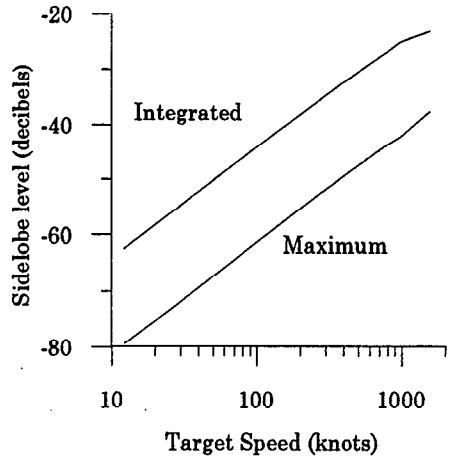

Figure 9. Maximum and integrated sidelobe levels as a function of target velocity. 33 point binomial weighted smoothing. Intermediate points calculation. $M = 1401$. $N = 201$.

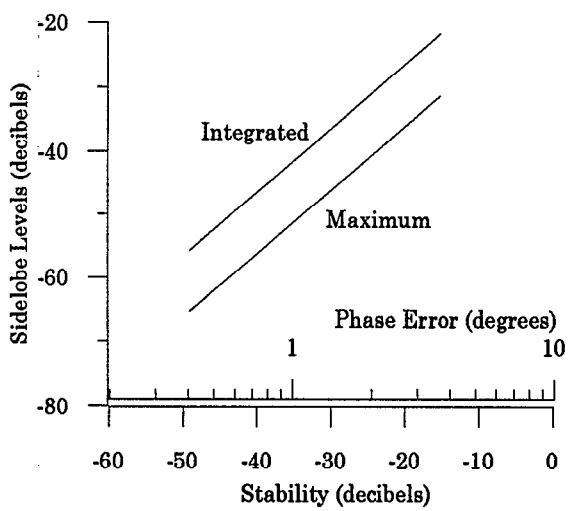

Figure 10. Maximum and integrated sidelobe levels as a function of transmitter phase error or stability. 33 point binomial weighted smoothing. Intermediate points calculation. $M = 1401$. $N = 201$.

5. Conclusion and Comments

We have shown how one can obtain low side lobes and how they are affected by various parameters. In particular, the deleterious effects of filter misalignment and its resolution by the use of receiver narrow banding has been analyzed and discussed. In the ASR radar context, there is no problem in handling mismatch losses or transmitter stability. However the sidelobes rapidly rise with target Doppler velocity. The configuration presented here limits the sidelobe level to about 50 dB for fast moving commercial jets. Furthermore, it has been shown recently[4] that the integrated and peak sidelobe levels are adequate most of the time for weather detection and other weather functions.

The computer program contains many input parameters. It is not clear that the best choice of parameters were made. It takes time and patience to converge to an acceptable solution. It is believed that the use of the binomial weighting function and the $\cos^2$ function for the transmitted spectrum are not critical. Other similar functions should work. However, the methods presented above are general enough to be used to assess the performance of proposed non-linear FM waveform radars.

REFERENCES

1. E.N.Fowle, *The Design of FM Pulse Compression Signals,* IEEE Trans. on Information Theory, Jan 1964.

2. S.Treitel and E.A.Robinson, *The Design of High Resolution Digital Filters,* IEEE Trans. on Geoscience Electronics, Vol. GE-4, No. 1, June 1966.

3. N.Levinson, Appendix B of N.Wiener, *Extrapolation, Interpolation, and Smoothing of Stationary Time Series*, New York: Wiley, 1949.

4. M.E.Weber, S.W.Troxel, *Assessment of the Weather Detection Capability of an ASR with Solid-State Transmitter*, Lincoln Laboratory Project Report ATC-209, 24 Feb 1994.